WAVEFORM SCHEDULING IN WIDEBAND ENVIRONMENTS

Sandeep P. Sira, Antonia Papandreou-Suppappola

Department of Electrical Engineering
Arizona State University

Darryl Morrell

Department of Engineering
Arizona State University

ABSTRACT

The time-variation due to Doppler scaling effects, coupled with scattering due to multipath propagation, can severely limit the performance of wideband systems. In this paper, we examine the dynamic configuration of transmitted waveforms for agile sensing to increase tracking performance in wideband environments. Using wideband frequency modulated waveforms, we present an algorithm for predicting the mean square tracking error and selecting the waveform that minimizes it in a target tracking application with a nonlinear observations model. The algorithm is based on the Cramér-Rao lower bound on the measurement errors that is computed using the wideband ambiguity function. Using simulations, we demonstrate the improved performance provided by scheduling over fixed configurations.

1. INTRODUCTION

In target tracking systems, the advent of waveform-agile sensors, that can shape their transmitted waveforms on-the-fly, has allowed the consideration of adaptive waveform configuration schemes [1]-[3]. These schemes seek the best suited waveform for each transmission so as to obtain information that best improves the estimate of the target state. The resulting system level optimization yields better tracking performance than when the sensors and the tracker are optimized independently.

Two simplifications are commonly assumed in the scenarios studied in the recent past: linear observation models and narrowband signal processing. Linear observation models permit the use of the Kalman filter as the tracker and, consequently, the derivation of optimal solutions to the waveform scheduling problem [1],[2]. The introduction of a nonlinear observations model necessitates the use of suboptimal filtering methods and significantly complicates the dynamic waveform selection problem [4]. For narrowband processing, approximations are made to the changes caused by the environment on the transmitted waveforms. The effect of the relative motion between the target and the observation platform manifests itself as a Doppler scaling (time dilation/ compression) on the waveform. Transmitted waveforms are treated as narrowband signals if this effect may be approximated by a simple frequency shift. The approximation is valid only when the time-bandwidth product (TB) of the waveform satisfies TB $\ll c/(2\dot{r})$, where c is the velocity of propagation and $\dot{r}$ is the range-rate or radial velocity of the target with respect to the observation platform [5]. In the case of radar, this condition is easily met as the velocity of propagation is very large ($c \approx 3\text{x}10^8$ m/s). In sonar applications however, $c \approx 1500$ m/s, and with velocities on the order of 10 m/s, we require TB $\ll 75$ to justify the narrowband assumption. As the TB of sonar signals is generally much higher than 100, wideband processing has to be used.

In this paper, we consider adaptive sensor configuration for wideband environments. We develop a configuration algorithm that utilizes the wideband ambiguity function of the transmitted waveform to dynamically select the signal that minimizes the predicted mean squared error (MSE) in the estimate of the target's range and range-rate. We demonstrate the performance of this computationally efficient algorithm using waveforms with varying time-frequency signatures.

2. WIDEBAND SIGNAL MODEL

We consider the problem of two sensors tracking a target in a wideband environment using wideband signals. Specifically, at each sampling instant, sensors A and B transmit a frequency-modulated (FM) chirp waveform

$$s(t) = a(t) \exp\{j2\pi(b\xi(t/t_r) + f_c t)\}, \qquad (1)$$

where $\xi(t/t_r)$ is a real valued phase function, b is the chirp rate, $t_r > 0$ is a normalization time value, and f_c is the carrier frequency. The amplitude envelope is given by

$$a(t) = \begin{cases} \frac{\alpha}{t_f}(t - \frac{T}{2} - t_f), & -T/2 - t_f \le t < -T/2 \\ \alpha, & -T/2 \le t < T/2 \\ \frac{\alpha}{t_f}(\frac{T}{2} + t_f - t), & T/2 \le t < T/2 + t_f, \end{cases}$$

where $\alpha \in \Re$ is chosen such that $s(t)$ in (1) has unit energy. The finite rise/fall time of $a(t)$ is $t_f \ll T/2$. Note that we

This work was supported by the Department of Defense, Grant No. AFOSR FA9550-05-1-0443 and the Fulton School of Engineering, Arizona State University.

use a trapezoidal envelope in (1) to permit the evaluation of the Cramér-Rao lower bound (CRLB) in Section 3. The waveform transmitted by sensor i = A, B, at time k, is parameterized by $\boldsymbol{\theta}_k^i = [\xi_k^i \ \lambda_k^i \ b_k^i]^{\mathrm{T}}$, where $\lambda = T + 2t_f$ is its duration.

When the transmitted signal reflects off a target, it undergoes a Doppler scaling depending on the target's velocity, and it is received after a time delay proportional to the target's range [5]. The received signal is given by

$$r(t) = \beta s\left(\sigma t - \tau\right) + n(t) \tag{2}$$

where $n(t)$ is the added noise, β is a complex constant accounting for attenuation and reflection, $\sigma = (c - \dot{r})/(c + \dot{r}) > 0$ is the Doppler scale, and $\tau = 2r/(c+\dot{r})$ is the delay. The range and range-rate of the target are r and $\dot{r}$, respectively. Since $\dot{r} \ll c$, we have $r \approx c\tau/2$ and $\dot{r} \approx c(1-\sigma)/2$.

3. WIDEBAND ENVIRONMENT MODEL

We seek to recursively estimate the two-dimensional (2-D) motion of a target described by $\mathbf{X}_k = [x_k \ \ y_k \ \ \dot{x}_k \ \ \dot{y}_k]^{\mathrm{T}}$, where x_k and y_k correspond to the position, and $\dot{x}_k$ and $\dot{y}_k$ to the velocity at time k in Cartesian coordinates. The observations of the target state consist of range and range-rate measurements, obtained from the two sensors. At time k, the sensors measure $h(\mathbf{X}_k) = [r_k^A \ \dot{r}_k^A \ r_k^B \ \dot{r}_k^B]^{\mathrm{T}}$, where

$$\begin{aligned} r_k^i &= \sqrt{(x_k - x^i)^2 \ + \ (y_k - y^i)^2} \\ \dot{r}_k^i &= (\dot{x}_k(x_k - x^i) + \dot{y}_k(y_k - y^i))/r^i \end{aligned}$$

for i = A, B, and sensor i is located at (x^i, y^i). The target dynamics are modeled by a linear, constant velocity model. The state-space model is then given by

$$\mathbf{X}_k = F\,\mathbf{X}_{k-1} + \mathbf{W}_k, \quad \mathbf{Z}_k = h(\mathbf{X}_k) + \mathbf{V}_k \ , \tag{3}$$

where $\mathbf{Z}_k$ represents the observation. The process and observation noise are modeled by the uncorrelated Gaussian sequences, $\mathbf{W}_k$ and $\mathbf{V}_k$, respectively. The constant matrix F and the process noise covariance Q are given by

$$F = \begin{bmatrix} 1 & 0 & \delta t & 0 \\ 0 & 1 & 0 & \delta t \\ 0 & 0 & 1 & 0 \\ 0 & 0 & 0 & 1 \end{bmatrix}, \ Q = q \begin{bmatrix} \frac{\delta t^3}{3} & 0 & \frac{\delta t^2}{2} & 0 \\ 0 & \frac{\delta t^3}{3} & 0 & \frac{\delta t^2}{2} \\ \frac{\delta t^2}{2} & 0 & \delta t & 0 \\ 0 & \frac{\delta t^2}{2} & 0 & \delta t \end{bmatrix}$$

where δt is the sampling interval and q is a constant.

The observation noise covariance depends on the resolution properties of the transmitted waveform and is given by $N(\boldsymbol{\theta}_k)$. Here, $\boldsymbol{\theta}_k = [\boldsymbol{\theta}_k^{A^{\mathrm{T}}} \boldsymbol{\theta}_k^{B^{\mathrm{T}}}]^{\mathrm{T}}$ is a combined waveform parameter vector for both sensors at time k. To obtain this matrix, we note first that the estimation of the parameters τ and σ, of the received signal in (2), is performed by filters matched to several possible values of delay and Doppler scale. The magnitude squared output of the filters provides the correlation between the received and transmitted signals at several points in the delay-Doppler scale plane. The filter outputs thus depend upon the correlation properties of the signal with delayed and dilated/compressed versions of itself. This correlation is characterized by the wideband ambiguity function (WAF) [6]

$$\mathrm{WAF}_s(\tau, \sigma) = \sqrt{\sigma} \int_{-\infty}^{\infty} s(t) s^*(\sigma t - \tau) dt.$$

Under the condition of high signal-to-noise ratio (SNR), the sidelobes of the WAF may be neglected and the location of its peak can provide an estimate of τ and σ. To obtain the CRLB on the errors of this estimation process, we first obtain the 2x2 Fisher Information matrix I whose elements are given by the second derivatives of the WAF at the true target delay and Doppler scale. For the waveform in (1), these elements are given by [7]

$$\begin{aligned} I_{1,1} &= \int_{-\lambda/2}^{\lambda/2} (\dot{a}^2(t) + a^2(t)\Omega^2(t)) dt - \\ &\quad \left[\int_{-\lambda/2}^{\lambda/2} a^2(t)\Omega(t) dt\right]^2 \\ I_{1,2} &= \int_{-\lambda/2}^{\lambda/2} t(\dot{a}^2(t) + a^2(t)\Omega^2(t)) dt - \\ &\quad \int_{-\lambda/2}^{\lambda/2} a^2(t)\Omega(t) dt \cdot \int_{-\lambda/2}^{\lambda/2} t a^2(t)\Omega(t) dt \\ I_{2,2} &= \int_{-\lambda/2}^{\lambda/2} t^2(\dot{a}^2(t) + a^2(t)\Omega^2(t)) dt - \\ &\quad \left[\int_{-\lambda/2}^{\lambda/2} t a^2(t)\Omega(t) dt\right]^2 - \frac{1}{4} \ , \end{aligned}$$

where $\Omega(t) = 2\pi(b\frac{d}{dt}\xi(t/t_r) + f_c)$, and $I_{2,1} = I_{1,2}$. In a matched filter receiver, the maximum likelihood estimates are jointly asymptotically Gaussian with covariance that approaches the CRLB [5]. Since we consider high SNR, perfect detection and no clutter, we assume that the receiver achieves the CRLB. For sensor i, the CRLB on the estimation of $[r_k \ \ \dot{r}_k]^{\mathrm{T}}$ is then given by $N(\boldsymbol{\theta}_k^i) = \Gamma I_k^{i\,-1} \Gamma^{\mathrm{T}} / \eta_k^i$ where $\Gamma = \mathrm{diag}(c/2, c/2)$ and η_k^i is the SNR. Furthermore, assuming that the measurement noise at each sensor is independent, $N(\boldsymbol{\theta}_k) = \mathrm{diag}(N(\boldsymbol{\theta}_k^A), N(\boldsymbol{\theta}_k^B))$.

4. DYNAMIC WAVEFORM SELECTION

The dynamic selection of the transmission waveform at time k is performed by predicting the MSE based on the current state estimate and the state-space model (3), and searching

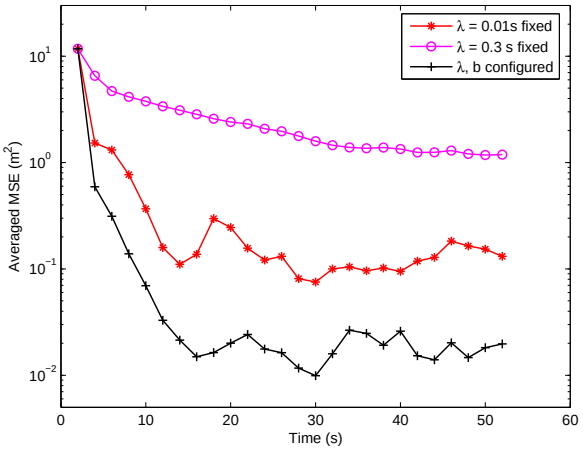

Fig. 1. Averaged MSE when both sensors use HFM chirps. The fixed waveforms had a frequency sweep of 2 kHz.

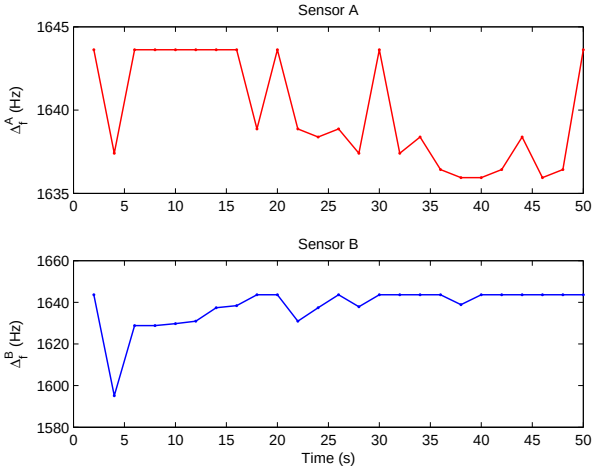

Fig. 2. Dynamic selection of the frequency sweep Δ_f^i, when both sensors i = A, B use HFM waveforms. The duration selected by both sensors at each sampling instant was 0.3 s.

for the waveform that minimizes it. We define the cost function as

$$J(\boldsymbol{\theta}_k) = E_{\mathbf{X}_k,\mathbf{Z}_k|\mathbf{Z}_{1:k-1}}\left\{(\mathbf{X}_k - \hat{\mathbf{X}}_k)^T \boldsymbol{\Lambda} (\mathbf{X}_k - \hat{\mathbf{X}}_k)\right\}, \tag{4}$$

and seek the value of $\boldsymbol{\theta}_k$ that minimizes it. Here, $E\{\cdot\}$ is the expectation over the predicted states $\mathbf{X}_k$ and observations $\mathbf{Z}_k$, and $\hat{\mathbf{X}}_k$ is the estimate of $\mathbf{X}_k$ given the sequence of observations from 1 to k. $\boldsymbol{\Lambda}$ is a weighting matrix that ensures that the units of the cost function are consistent.

Due to the nonlinear relationship between the observations and the target state, we use a particle filter to recursively estimate the probability distribution of the state given the sequence of observations, $p(\mathbf{X}_k|\mathbf{Z}_{1:k}, \boldsymbol{\theta}_{1:k})$. The conditional mean of this density yields the state estimate. The cost function in (4) cannot be computed in closed form since the estimate $\hat{\mathbf{X}}_k$ can only be obtained by simulation. Although it is possible to compute the cost by Monte Carlo methods, it is computationally expensive. Instead, we use a method based on the unscented transform (UT) [8] to predict the MSE and perform a grid search. The search progressively explores finer regions of the space of allowable waveforms and waveform parameters to determine the waveform that minimizes the predicted MSE [4].

Specifically, at time $k-1$, the UT is used to obtain the predicted covariance matrices of the state and the observation as $P_{xx}(k|k-1)$ and P_{zz}, respectively, and their cross covariance P_{xz}. For the lth waveform with parameter vector $\boldsymbol{\theta}_k(l)$, $l = 0, \ldots, L-1$, the updated predicted MSE is

$$P_{xx}^l(k|k) = P_{xx}(k|k-1) - P_{xz}\left[P_{zz} + N(\boldsymbol{\theta}_k(l))\right]^{-1} P_{xz}^{\mathrm{T}},$$

and $J(\boldsymbol{\theta}_k^l)$ is approximated by the trace of $\boldsymbol{\Lambda} P_{xx}^l(k|k)$. The configuration $\boldsymbol{\theta}_k(l)$ that minimizes the cost function is then applied to the sensors to obtain the observation $\mathbf{Z}_k$.

5. SIMULATIONS AND DISCUSSION

The simulation study to test the performance of the waveform scheduling algorithm in a wideband environment involved two waveform-agile sensors tracking an underwater target moving in 2-D, using range and range-rate measurements. The carrier frequency of the transmitted waveform was $f_c = 25$ kHz and the waveform duration ranged within 0.01 s $\leq \lambda \leq$ 0.3 s. The SNR at sensor i at time k was determined according to $\eta_k^i = (r_0/r_k^i)^4$, where $r_0 = 500$ m was the range at which 0 dB SNR was obtained. We considered a number of FM chirps with different time-frequency signatures that are specified by their phase functions, $\xi(t/t_r)$ in Table 1 with $t_r = 1$. We define the frequency sweep to be $\Delta_f^i = |\Omega^i(\lambda^i/2) - \Omega^i(-\lambda^i/2)|$, where $\Omega^i(t)$ is the instantaneous frequency, and limit it to a maximum of 2 kHz. We fix $\Omega^i(-\lambda^i/2) = f_c + 2$ kHz (downswept chirps) or $\Omega^i(\lambda^i/2) = f_c + 2$ kHz (upswept chirps). We then compute b^i and T_f^i in Table 1 for each waveform for any chosen frequency sweep. The sampling interval and the process noise intensity in (3) were $\delta t = 2$ s and $q = 0.01$, respectively. The speed of sound in water was taken as $c = 1500$ m/s.

In the first example, we configured each sensor with the hyperbolic FM (HFM) waveform and dynamically selected its parameters (λ and b) for each sensor so as to minimize the predicted MSE. The actual MSE obtained in tracking a target, averaged over 500 simulations, is shown in Fig. 1. For comparison, we also show the MSE that was obtained when the sensor configurations were fixed at the minimum or maximum durations and the maximum frequency sweep. The improvement in performance in using dynamic parameter selection is apparent. Fig. 2 shows the dynamic selection of the frequency sweep that results from the selection of the chirp rate b^i by the configuration algorithm. Note that the

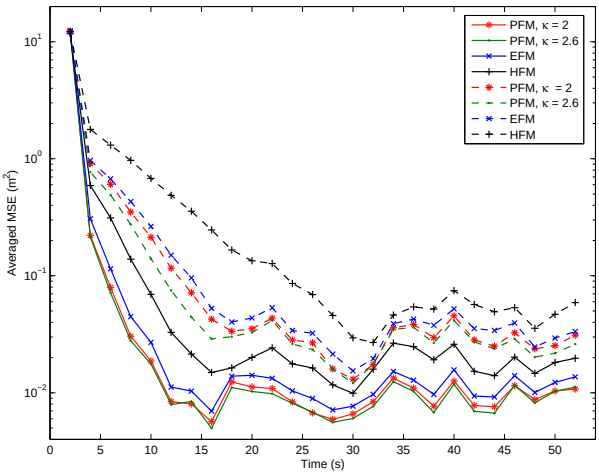

Fig. 3. Comparison of averaged MSE using various waveforms when the allowed frequency sweep is 1 kHz (dotted) and 2 kHz (solid).

frequency sweep chosen by dynamically selecting the chirp rate is much less than the maximum of 2 kHz. The pulse duration was always selected as the maximum of 0.3 s.

In the second simulation example, we permitted the sensors to dynamically select the phase function from among the options in Table 1. We allowed the waveform selection to choose between hyperbolic, exponential, and power FM chirps with $\kappa = 2$ and 2.6, in addition to choosing the duration λ and chirp rate b so as to minimize the predicted MSE. Fig. 3 plots the averaged MSE when dynamic parameter selection is used with FM waveforms with different phase functions. Note that the power FM (PFM) chirp with $\kappa = 2$ constitutes a linear FM chirp. From Fig. 3, the PFM chirp with $\kappa = 2.6$ performs the best and we should expect that it will always be chosen as it was indeed observed.

The HFM chirp yielded the poorest performance as seen in Fig. 3. It has been shown that the HFM chirp is optimally Doppler tolerant [7]. This also implies that it is minimally Doppler sensitive and should compare poorly with the tracking performance of other FM waveforms.

As the variance of the range-rate estimation errors depends inversely on the pulse duration, the algorithm attempts to minimize these errors when the maximum allowed pulse length is used. On the other hand, range estimation errors can be minimized by using the maximum TB. However, the correlation between the errors increases with increasing frequency sweep, thereby reducing the ability of the waveform to estimate range and range-rate *simultaneously*. Thus, there is a tradeoff in the choice of frequency sweep and this is reflected in the selections made by the configuration algorithm as it responds to the tracker's current estimate of the target state. The performance also improves with increasing frequency sweep.

Waveform	Phase Function, $\xi(t)$ in (1)
Power FM (PFM)	$t/T_f + (t + \lambda/2)^\kappa/\kappa$
Hyperbolic FM (HFM)	$\ln(t + T_f + \lambda/2)$
Exponential FM (EFM)	$\exp\{-(t + \lambda/2)/T_f\}$

Table 1. FM waveforms used in the configuration.

6. CONCLUSION

The requirement to utilize wideband processing methods is especially acute in applications where the velocity of propagation of the waveform is low and its time-bandwidth product is large. The optimization of tracking systems is further complicated by nonlinear observation models that necessitate sub-optimal filters. In this paper, we presented an algorithm to configure waveform-agile sensors on-the-fly to reduce the tracking MSE. The algorithm uses the CRLB to determine the effect of choosing a particular waveform on the tracking performance, while the UT is used to compute the MSE efficiently. The configuration algorithm searches the available space of waveforms to find the one that yields the lowest predicted MSE. We implemented a simulation study using FM waveforms with different time-frequency signatures. The results indicate that dynamic sensor configuration provides improvements in performance over fixed configurations.

7. REFERENCES

[1] D. J. Kershaw and R. J. Evans, "Optimal waveform selection for tracking systems," *IEEE Transactions on Information Theory*, vol. 40, pp. 1536–1550, Sep. 1994.

[2] S. Hong, R.J. Evans, and H. Shin, "Optimization of waveform and detection threshold for range and range-rate tracking in clutter," *IEEE Trans. on Aerospace and Electronic Systems*, vol. 41, no. 1, pp. 17–33, Jan. 2005.

[3] S. D. Howard, S. Suvorova, and W. Moran, "Waveform libraries for radar tracking applications," *International Conference on Waveform Diversity and Design*, Nov. 2004.

[4] S. P. Sira, A. Papandreou-Suppappola, and D. Morrell, "Time-varying waveform selection and configuration for agile sensors in tracking applications," *ICASSP*, vol. 5, pp. 881–884, March 2005.

[5] H. L. Van Trees, *Detection Estimation and Modulation Theory, Part III*, Wiley, New York, 1971.

[6] D. A. Swick, "A review of wideband ambiguity functions," Tech. Rep. 6994, NRL, Washington, D.C., Dec. 1969.

[7] R. A. Altes and E. L. Titlebaum, "Bat signals as optimally Doppler tolerant waveforms," *Journal of the Acoustical Society of America*, vol. 48, no. 4B, pp. 1014–1020, Oct. 1970.

[8] S. Julier and J. Uhlmann, "A new extension of the Kalman filter to nonlinear systems," *International Symposium on Aerospace/Defense Sensing, Simulation and Controls*, 1997.